Progress in Neuropsychopharmacology & Biological Psychiatry 79 (2017) 302–310

Contents lists available at ScienceDirect

Progress in Neuropsychopharmacology & Biological Psychiatry

journal homepage: www.elsevier.com/locate/pnp

Common and distinct dysfunctional patterns contribute to triple network model in schizophrenia and depression: A preliminary study

Yuchao Jiang[a,1], Mingjun Duan[a,b,1], Xi Chen[a], Xin Chang[a], Hui He[a], YingJia Li[a], Cheng Luo[a,*], Dezhong Yao[a,*]

[a] Key Laboratory for NeuroInformation of Ministry of Education, Center for Information in Medicine, High-Field Magnetic Resonance Brain Imaging Key Laboratory of Sichuan Province, School of Life Science and Technology, University of Electronic Science and Technology of China, Chengdu, China
[b] Department of psychiatry, Chengdu Mental Health Center, Institute of Chengdu Brain Science, Chengdu, China

ABSTRACT

Background: Schizophrenia (SCH) and depression (DEP) are prevalent psychiatric disorders and share common and distinguished elements in their pathophysiology. A triple network model composed of the default mode network (DMN), salience network (SN) and central executive network (CEN) may represent a major abnormality across several psychiatric disorders including SCH and DEP. However, common and distinct dysfunctional patterns between SCH and DEP across three core networks remain unclear.

Method: Resting-state functional magnetic resonance imaging (fMRI) was obtained in 20 patients with SCH, 20 patients with DEP and 20 healthy controls (HC). Both functional connectivity (FC) and Granger causal connectivity across DMN, SN and CEN were evaluated to uncover common and distinct dysfunctional patterns between SCH and DEP.

Results: Two patient groups showed identical abnormal causal connectivity between key nodes of DMN and SN, as well as opposing aberrant FC of DMN-CEN and SN-CEN. Compared with HC, the FC between CEN and DMN was increased in SCH while decreased in DEP. Conversely, DEP showed enhanced FC between CEN and SN, whereas SCH showed decreased FC.

Limitations: The sample size was relatively small, and all participants were taking medication.

Conclusions: Our results identified common patterns including dysconnectivity between DMN and SN, which may contribute to shared cognitive and affective impairment in DEP and SCH. Moreover, opposing dysconnectivity patterns of DMN-CEN may be associated with different self-referential processing abnormalities. These opposing dysconnectivity patterns may indicate an unbalanced recruitment between SN and CEN. Therefore, this study provides dysconnectivity patterns to advance the understanding of the triple network model with regard to psychiatric disorders.

1. Introduction

Schizophrenia (SCH) and depression (DEP) are two serious psychiatric disorders that have both common and distinct clinical features. For example, both diseases share many common characteristic symptoms and signs such as cognitive and affective impairment. Moreover, self-referential processes are altered in patients with SCH (van der Meer et al. 2010) and those with DEP (Sheline et al. 2009) but have distinct manifestations. SCH is characterized by a typically reduced level of self-reference, whereas DEP is characterized by extensive self-attribution.

Resting-state functional magnetic resonance imaging (fMRI) studies have shown that the disruption of the coordinated activity of multiple brain networks is crucial for various pathological psychiatric conditions (Dong et al. 2017; Duan et al. 2015; Menon 2011). Specifically, previous studies have focused on disturbances in three important networks: the central executive network (CEN), the salience network (SN) and the default mode network (DMN) (Whitfield-Gabrieli and Ford 2012). The CEN, a frontoparietal system that includes the dorsolateral prefrontal cortex (DLPFC) and inferior parietal lobule (IPL) (Seeley et al. 2007), is crucial for manipulating information about the external environment. The DMN, which includes the posterior cingulate cortex (PCC), medial prefrontal cortex (MPFC), angular gyrus and medial temporal gyrus, plays an important role in monitoring self-referential mental processes (Luo et al. 2011). The SN, which is composed of the

* Corresponding authors at: University of Electronic Science and Technology of China, Second North Jianshe Road, Chengdu 610054, China.
E-mail addresses: chengluo@uestc.edu.cn (C. Luo), dyao@uestc.edu.cn (D. Yao).
[1] These authors contributed equally to this work.

http://dx.doi.org/10.1016/j.pnpbp.2017.07.007
Received 23 December 2016; Received in revised form 5 July 2017; Accepted 8 July 2017
Available online 10 July 2017

anterior insula, dorsal anterior cingulate cortex (dACC) and temporoparietal junction (TPJ), is involved in detecting, filtering and integrating relevant salient external stimuli and interoceptive signals (Seeley et al. 2007). As such, a triple network model that synthesizes the extant findings regarding these networks has been proposed to understand pathophysiological dysfunction across several psychiatric disorders (Menon 2011). In this model, dysfunction in one network may affect the other two. In addition, the abnormal integration of information within and across these networks is important in linking the concomitant impaired cognitive features characteristic of psychopathology (Pessoa 2008). An aberrant organization among the three networks might also be associated with abnormal interactions between external stimuli and internal events with regard to self-referential processes (Menon and Uddin 2010). Therefore, additional investigations of the disruptions across core networks are necessary to advance the understanding of the fundamental brain mechanisms that underlie psychopathology.

SCH and DEP have been generally identified in relation to the aberrant functioning and organization of the CEN, SN and DMN (Nekovarova et al. 2014). However, whether common and distinct dysfunctional patterns exist across three networks with regard to SCH and DEP remains unclear. Here, we speculate that identical and opposite aberrant connectivity patterns exist across the three core networks in patients with SCH and those with DEP. Exploring the identical and opposite dysconnectivity patterns could not only help to characterize the dynamic interaction and functional integration of information across the core networks, but also enhance the insights concerning the shared and disparate psychopathologies that underlie the abnormalities in the triple network model with regard to patients with SCH or DEP.

To test our hypothesis, we used the functional connectivity (FC) analysis and Granger causal analysis (GCA) (Hamilton et al. 2011) to investigate the undirected and directed connectivity across the DMN, SN and CEN. In addition, we evaluated whether the altered connectivity in patients is correlated with certain clinical variables.

2. Methods

2.1. Participants

Twenty patients with SCH diagnosed using the Diagnostic and Statistical Manual of Mental Disorders, Fourth Edition (DSM-IV), 20 patients with DSM-IV major depressive disorder, and 20 healthy controls (HC) were recruited from Chengdu Mental Health Centre. Participants with histories of major neurological disorders, brain structural abnormalities or substance-related disorders were excluded. A history of a psychiatric disorder in a first- or second-degree relative was an additional exclusion criterion. None of the patients with SCH had a history of a major depressive episode. Written informed consent was obtained after the study was completely described to each participant. The study was approved by the Ethics Committee of Chengdu Mental Health Centre. Symptom severity was assessed using the Positive and Negative Syndrome Scale (PANSS) and the 24-item Hamilton Rating Scale for Depression (HAMD-24) for patients with SCH and those with DEP, respectively. All patients were taking medication (e.g., antidepressants and neuroleptics). Medication use almost perfectly aligned with the patients' diagnostic categories (Supplement 1).

2.2. Image acquisition

A 3-Tesla MRI scanner (GE DISCOVERY MR 750, USA) was used to collect imaging data at the Centre for Information in Medicine of the University of Electronic Science and Technology of China. The gradient-echo echo-planar imaging (EPI) sequence was used to acquire the functional images. The main scan parameters were as follows: TR/TE = 2 s; TE = 30 ms; flip angle = 90°; field of view = 24 cm × 24 cm; matrix size = 64 × 64; slice thickness = 4 mm (no gap), slice = 35. All participants were instructed to relax and close their eyes without falling asleep. Each functional resting-state session lasted 510 s, resulting in 255 volumes. All of these datasets were also included in our previous study (Chen et al. 2017), in which the target was other than the current study.

2.3. Data preprocessing

The data preprocessing steps included (1) removing the first five time points for signal equilibrium and to allow the participants to adapt to the scanning noise; (2) slice timing; (3) realignment; (4) coregistering the individual T1 image to the functional space and segmenting; (5) nuisance signal regression (including Friston 24-parameter motion correction (Satterthwaite et al. 2013), five CompCorr signals (Chai et al. 2012) of white matter and cerebrospinal fluid (CSF), and linear trend); (6) temporal scrubbing using the "bad" time points (frame-wise displacement (FD) (Power et al. 2012) > 0.5) as a regressor; (7) normalizing to MNI space ($3 \times 3 \times 3\ mm^3$) using segment information; (8) band-pass filtering (0.01–0.1 Hz); and (9) smoothing (FWHM = 4 mm). The unsmoothed data was used in the cluster analysis to avoid blurring between insular subregions (Moran et al. 2013). The global mean signal was not regressed out because it may distort between-group comparisons of inter-regional correlation (Saad et al. 2012). In addition, we also compared the differences of various head-motion parameters between groups (Supplement 2).

2.4. Definition of the triple network

The seed-based FC analysis was used to identify the three core networks. The 8-mm spheres of the DLPFC (48,18,17) (Whitfield-Gabrieli et al. 2009) and PCC (−5,−49,40) (Fox et al. 2005) were defined as the seed regions for the CEN and DMN. However, a functional parcellation was used to identify the seed of the SN because the signal of insular subregions might be effected by the CSF and vessel in lateral fissure. In general, the insula can be divided into three subregions: the dorsal anterior insula [dAIns], ventral anterior insula [vAIns] and posterior insula [PIns]. The right dAIns was selected as the seed to define the SN (Touroutoglou et al. 2012). Here, we functionally parcellated the right insula into three regions using an identified method (Supplement 3) same as our previous studies (Cao et al. 2016; Chen et al. 2016), and chose the dAIns as the seed. Then, whole brain voxel-wise Pearson's correlation analyses were used to define the masks of the SN, CEN and DMN separately. In detail, Fisher-Z-transformed correlation coefficients [z(r)] were computed between the average time series of each seed and the whole brain voxels. Finally, one-tailed one sample *t*-tests were performed to determine the significant connectivity with seed (Touroutoglou et al. 2012). Multiple comparisons correction for all FC analyses was performed with an individual p of 0.001 and a minimum cluster size based on Gassian Random Field (GRF) theory, which corresponds to $P_{corrected} = 0.05$. Thus, the voxels positively correlated with the seeds were considered including the three networks.

2.5. Voxel-wise functional connectivity and effective connectivity analyses

For the FC analysis, the Z-transformed coefficient mentioned above was further analyzed in the union mask of CEN, SN and DMN to investigate the undirected FC among the three groups.

For the effective connectivity analysis, the seed-based voxel-wise GCA was performed with regard to the mask of the CEN, SN and DMN with three seeds: dAIns, DLPFC and PCC. First, we used a vector autoregression (i.e., Granger) approach that examined the time lagged effects between two nodes to infer the causal effects between regions (Chen et al. 2011). The signed-path coefficient generated using a time lag order of 1 TR (2 s) was used to estimate the probable excitatory or inhibitory effect of the directed physiological influence (Hamilton et al. 2011; Zang et al. 2012). The bivariate GCA accounted for the

physiological probability of simultaneously bidirectional influences in the brain (Palaniyappan et al. 2013). In addition, the path coefficients were normally distributed and could be used in parametric statistical analysis for group level inference (Hamilton et al. 2011).

To investigate the effect of group and differences between groups, a 3-level ANCOVA and post-hoc LSD tests were performed on the FC and GCA maps with sex, age and education as unconcerned covariates, respectively. In addition, head-motion variables were treated as extra covariates. Multiple comparisons correction was performed using GRF correction ($P_{corrected} < 0.05$).

To better characterize the common and distinct dysfunctional modulation across the three networks between patients with SCH and those with DEP, we emphasized two typical abnormal connectivity: common and distinct dysfunction. Common dysfunction between two diseases is the identical altered connectivity that meets the following conditions: (1) both patient groups significantly differ from the HC, and (2) the two patient groups did not significantly differ from each other. Considering that this situation may arise from the insufficient statistical power associated with small sample sizes, a power analysis was further conducted (Supplement 4). The distinct dysfunction is the opposite altered connectivity that satisfies that (1) both patient groups significantly differ from HC, (2) the two patient groups significantly differ from each other, and (3) relative to HC, the two patient groups exhibit the opposing changes.

2.6. Correlations between abnormal connectivity and clinical variables

We also investigated the relationships between altered connectivity and clinical features. The correlation analyses were performed separately for each patient group. In the SCH group, we estimated the relationships between altered connectivity and disease duration, medication dosage and PANSS (positive, negative, general psychopathology subscales and total scores). In the DEP group, we assessed the relationships between altered connectivity and disease duration as well as HAMD. The Kolmogorov-Smirnov tests were used to determine whether these variables were normally distributed. Then, partial correlations were performed after controlling for the effects of gender, age, education level and head-motion variables.

3. Results

3.1. Demographic and clinical variables

The demographic and clinical characteristics of the samples are presented in Table 1. Three groups showed no difference in terms of gender (chi-square test, $p = 0.754$), age (Kruskal-Wallis test, $p = 0.931$) and education (Kruskal-Wallis test, $p = 0.305$). Patients significantly differed with regard to disease duration (Mann-Whitney U test, $p = 0.016$). Both patient groups showed low symptomatology levels (HAMD score < 7 and PANSS total score < 60).

3.2. Definition of the three core networks

Consistent with previous studies (Chen et al. 2016), the dAIns exhibited a strong connection with the dACC, TPJ and ventrolateral prefrontal cortex (VLPFC). The DLPFC showed significant connectivity with the IPL, another key node of the CEN. Furthermore, the PCC was strongly connected with the other regions of the DMN, including the MPFC, angular, superior frontal cortex (SFC), inferior temporal cortex, and parahippocampal gyrus (Fig. 1 and Table S2). These areas that showed significant FC with the dAIns, DLPFC and PCC were separately defined as the mask of the SN, CEN and DMN.

3.3. Differences in functional connectivity among the three networks

For the seed of the right dAIns, a significant group effect of its FC with right IPL and right SFC was observed. For the seed of the right DLPFC, the ANCOVA exhibited a significant group effect in FC with left MPFC and precuneus. For the seed of the PCC, the ANCOVA demonstrated a significant group effect in FC with left pas opercularis of the inferior frontal cortex (OPIFC) and left pas triangularis of the inferior frontal cortex (TIFC). Interestingly, post-hoc analyses revealed an opposite altered FC pattern between key nodes of the CEN-DMN and CEN-SN for both patient groups (Fig. 2A). Patients with SCH showed a reduced FC between nodes of the SN and CEN (dAIns.R-IPL.R) compared with HC whereas patients with DEP showed enhanced FC. In addition, patients with SCH showed increased FC between the key nodes of the DMN and CEN (PCC-TIFC.R and MPFC.L-DLPFC.R) compared with HC whereas DEP patients showed decreased FC. Moreover, post-hoc analyses showed SCH-specific FC alterations in which these patients had higher FC (dAIns.R-SFC.L, DLPFC.R-Precuneus and PCC-OPIFC.L) than those with DEP and HC. All of the results from the ANCOVA and post-hoc analyses are presented in Table 2.

Table 1
Demographic and clinical characteristics.

	Schizophrenia (n = 20) Mean(SD)	Depression (n = 20) Mean(SD)	Healthy control (n = 20) Mean(SD)	P value
Gender(male/female)	9/11	7/13	7/13	0.754[a]
Age(years)	40.3(13.8)	41.8(14.2)	41.6(13.6)	0.931[b]
Education (years)	10.9(2.7)	11.3(2.6)	10.4(2.9)	0.305[b]
Disease duration (years)	13.3(9.6)	6.4(5.4)		0.016[c,*]
PANSS				
Positive score	12.9(5.6)			
Negative score	18.0(7.0)			
General score	27.8(5.3)			
Total score	58.8(12.5)			
HAMD-24		5.3(1.3)		

[a] Chi-square test.
[b] Kruskal-Wallis tests.
[c] Mann-Whitney were used to assess group differences for various variable types.
[*] $p < 0.05$.

3.4. Differences in effective connectivity among the three networks

For the seed of the SN (right dAIns), significant group differences in the causal connectivity from the right dAIns to the left middle frontal gyrus (MFG) and right precuneus were observed according to an ANCOVA. The post-hoc analyses revealed that both patient groups had a consistent decrease in the causal connectivity from the right dAIns to the PCC. However, only patients with SCH showed increased causal connectivity from the right dAIns to the left MFG and precuneus compared with HC.

For the seed of the CEN (right DLPFC), the ANCOVA revealed significant group differences in the causal outflow from the right DLPFC to the right angular and inflow from the left superior temporal cortex (STC) and right angular to the right DLPFC. The post-hoc analyses showed reduced causal connectivity from the right angular to the right DLPFC in patients with SCH but not those with DEP or HC.

For the seed of the DMN (PCC), the ANCOVA exhibited significant group differences with regard to the outflow from the PCC to the bilateral dAIns, TPJ and dACC as well as inflow from the right insula to the PCC. In particular, the post-hoc analyses showed an identical altered causal connectivity pattern from the PCC to the bilateral dAIns and TPJ within two patient groups (Fig. 2B). In detail, both patients with SCH and those with DEP exhibited significant increases in the causal connectivity from the PCC to the bilateral dAIns and TPJ

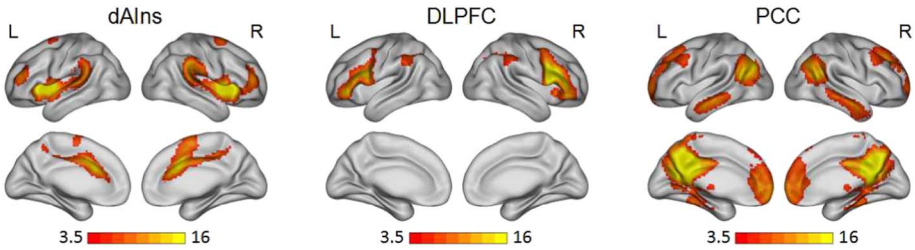

Fig. 1. T maps of functional connectivity with the seeds of the dorsal anterior insula (dAIns), dorsolateral prefrontal cortex (DLPFC) and posterior cingulate cortex (PCC). One-sample *t*-test was performed across all participants.

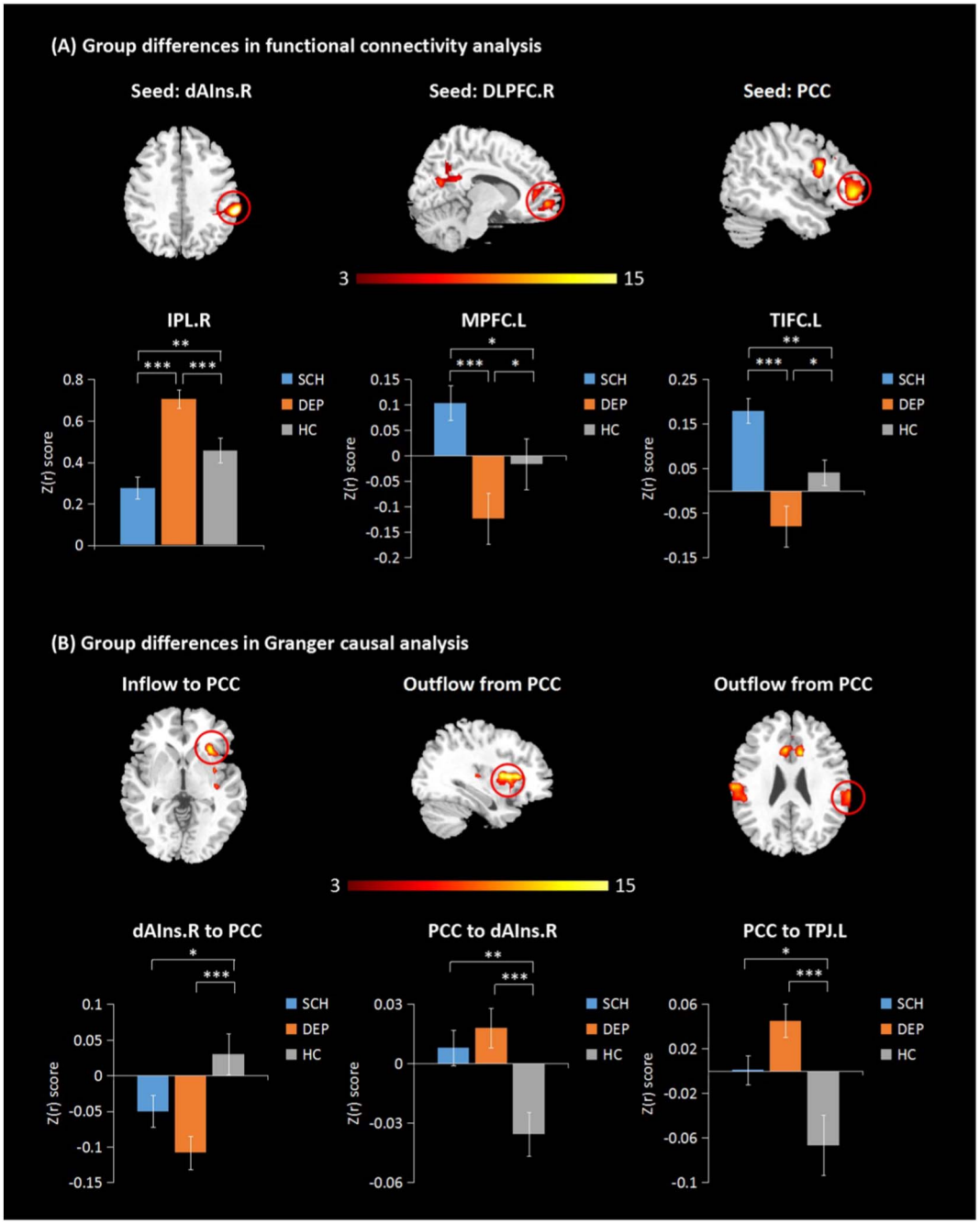

Fig. 2. Group differences among the SCH, DEP and HC groups in (A) functional connectivity analysis and (B) Granger causal analysis.
Abbreviations: L: left, R: right, dAIns: dorsal anterior insula, IPL: inferior parietal lobule, DLPFC: dorsolateral prefrontal cortex, PCC: posterior cingulate cortex, TPJ: temporoparietal junction.

Table 2
Functional connectivity differences among the SCH, DEP and HC groups.

Regions	MNI coordinates (x,y,z)	Mean(SE) correlation Coefficient			Main effect of ANCOVA			Post-hoc LSD test P value
		SCH	DEP	HC	F value	P value	Cluster-size	
Seed: dAIns								
IPL.R	63, − 36,39	0.28 (0.053)	0.71 (0.045)	0.46 (0.060)	23.6	5.3×10^{-8}	339	p(SCH < DEP) = $1.6 * 10^{-8}$* p(SCH < HC) = 7.1×10^{-3}* p(DEP > HC) = 3.0×10^{-4}*
SFC.R	15,42,36	− 0.12 (0.053)	− 0.39 (0.031)	− 0.33 (0.052)	11.0	1.1×10^{-4}	274	p(SCH > DEP) = 2.7×10^{-5}* p(SCH > HC) = 8.5×10^{-4}* p(DEP < HC) = 2.9×10^{-1}
Seed: DLPFC								
MPFC.L	− 15,57, − 3	0.10 (0.038)	− 0.12 (0.033)	− 0.02 (0.034)	12.0	5.2×10^{-5}	236	p(SCH > DEP) = 1.5×10^{-5}* p(SCH > HC) = 1.4×10^{-2}* p(DEP < HC) = 2.8×10^{-2}*
Precuneus.R	9, − 57,21	0.11 (0.047)	− 0.11 (0.039)	0.002 (0.045)	7.3	1.6×10^{-3}	326	p(SCH > DEP) = 5.0×10^{-4}* p(SCH > HC) = 7.2×10^{-2} p(DEP < HC) = 6.6×10^{-2}
Seed: PCC								
OPIFC.L	− 57,9,18	0.11 (0.052)	− 0.19 (0.047)	− 0.08 (0.044)	13.1	2.5×10^{-5}	237	p(SCH > DEP) = 8.0×10^{-6}* p(SCH > HC) = 2.6×10^{-3}* p(DEP < HC) = 7.9×10^{-2}
TIFC.L	− 42,36,0	0.18 (0.025)	− 0.08 (0.046)	0.04 (0.028)	14.1	1.3×10^{-5}	199	p(SCH > DEP) = 3.2×10^{-6}* p(SCH > HC) = 7.5×10^{-3}* p(DEP < HC) = 1.8×10^{-2}*

Abbreviations: L: left, R: right, dAIns: dorsal anterior insula, IPL: inferior parietal lobule, SFC: superior frontal cortex, DLPFC: dorsolateral prefrontal cortex, PCC: posterior cingulate cortex, OPIFC: pas opercularis of the inferior frontal cortex, TIFC: pas triangularis of the inferior frontal cortex.
* $p < 0.05$.

Table 3
Effective connectivity differences among the SCH, DEP and HC groups in the Granger causal analysis at the right dAIns.

Regions	MNI coordinates (x,y,z)	Mean(SE) path coefficient			Main effect of ANCOVA			Post-hoc LSD test P value
		SCH	DEP	HC	F value	P value	Cluster-size	
Causal outflow from the dAIns(x-to-y coefficients)								
MFG.L	− 18,30,36	0.030 (0.012)	− 0.040 (0.012)	− 0.012 (0.009)	10.9	1.1×10^{-4}	289	p(SCH > DEP) = 3.39×10^{-5}* p(SCH > HC) = 8.5×10^{-3}* p(DEP < HC) = 7.7×10^{-2}
Precuneus.R	6, − 54,39	0.016 (0.020)	− 0.106 (0.026)	− 0.050 (0.018)	7.3	1.7×10^{-3}	191	p(SCH > DEP) = 1.8×10^{-4}* p(SCH > HC) = 3.4×10^{-2}* p(DEP < HC) = 7.0×10^{-2}

Abbreviations: L: left, R: right, dAIns: dorsal anterior insula, MFG: middle frontal gyrus.
* $p < 0.05$.

Table 4
Effective connectivity differences among SCH, DEP and HC groups in the Granger causal analysis at the right DLPFC.

Regions	MNI coordinates (x,y,z)	Mean(SE) path coefficient			Main effect of ANCOVA			Post-hoc LSD test P value
		SCH	DEP	HC	F value	P value	Cluster-size	
Causal inflow to the DLPFC(y-to-x coefficients)								
STG.L	− 45, − 21, − 6	0.016 (0.009)	− 0.025 (0.008)	− 0.037 (0.013)	9.1	4.2×10^{-4}	154	p(SCH > DEP) = 6.0×10^{-3}* p(SCH > HC) = 5.0×10^{-4}* p(DEP > HC) = 4.0×10^{-1}
Ang.R	48, − 60,39	− 0.021 (0.009)	0.019 (0.006)	0.001 (0.005)	9.2	3.8×10^{-4}	166	p(SCH < DEP) = 1.2×10^{-4}* p(SCH < HC) = 2.6×10^{-2}* p(DEP > HC) = 6.5×10^{-2}

Abbreviations: L: left, R: right, DLPFC: dorsolateral prefrontal cortex, STG: superior temporal gyrus, Ang: angular.
* $p < 0.05$.

compared with HC. Patients with DEP showed significantly increased causal connectivity from the PCC to the dACC and decreased causal connectivity from the dACC to the PCC compared with SCH patients and HC. All of the results of the ANCOVA and post-hoc analyses are presented in Tables 3–5.

3.5. Correlations between abnormal connectivity and clinical variable

A total of 114 correlation analyses were performed in the SCH group (19 altered connections × six clinical variables). Twenty correlation analyses were applied for the DEP group (10 altered connections × two clinical variables). The partial correlation analysis showed that the causal connectivity from the PCC to the left TPJ was positively

Table 5
Effective connectivity differences among the SCH, DEP and HC groups in the Granger causal analysis at the PCC.

Regions	MNI coordinates (x,y,z)	Mean(SE) path coefficient			Main effect of ANCOVA			Post-hoc LSD test P value
		SCH	DEP	HC	F value	P value	Cluster-size	
Causal outflow from the PCC(x-to-y coefficients)								
dAIns.L	− 36,21,6	0.006 (0.004)	0.029 (0.010)	− 0.020 (0.010)	9.7	2.7×10^{-4}	515	p(SCH < DEP) = 9.5×10^{-2} p(SCH > HC) = 4.9×10^{-2}* p(DEP > HC) = 5.1×10^{-4}*
dAIns.R	33,6,3	0.008 (0.009)	0.018 (0.010)	− 0.036 (0.011)	10.1	2.0×10^{-4}	326	p(SCH < DEP) = 4.7×10^{-1} p(SCH > HC) = 2.7×10^{-3}* p(DEP > HC) = 3.0×10^{-4}*
TPJ.L	− 45, − 30,18	− 0.008 (0.011)	0.017 (0.011)	− 0.039 (0.011)	11.1	9.9×10^{-5}	515	p(SCH < DEP) = 8.6×10^{-2} p(SCH > HC) = 2.8×10^{-2}* p(DEP > HC) = 2.0×10^{-4}*
TPJ.R	51, − 30,9	0.001 (0.013)	0.045 (0.020)	− 0.067 (0.027)	9.0	4.3×10^{-4}	335	p(SCH < DEP) = 1.3×10^{-1} p(SCH > HC) = 2.1×10^{-2}* p(DEP > HC) = 2.5×10^{-4}*
dACC.Mid	3,9,36	0.005 (0.014)	0.085 (0.019)	− 0.028 (0.016)	12.5	3.8×10^{-5}	512	p(SCH < DEP) = 1.0×10^{-3}* p(SCH > HC) = 1.7×10^{-1} p(DEP > HC) = 1.3×10^{-5}*
Causal inflow to the PCC(y-to-x coefficients)								
dAIns.R	33,15,9	− 0.050 (0.022)	− 0.108 (0.023)	0.030 (0.030)	8.5	6.3×10^{-4}	189	p(SCH > DEP) = 1.0×10^{-1} p(SCH < HC) = 2.7×10^{-2}* p(DEP < HC) = 2.5×10^{-4}*
dACC.Mid	− 3,3,36	0.028 (0.013)	− 0.081 (0.014)	− 0.012 (0.017)	12.5	3.6×10^{-5}	398	p(SCH > DEP) = 4.2×10^{-6}* p(SCH > HC) = 6.5×10^{-2} p(DEP < HC) = 2.0×10^{-3}*

Abbreviations: L: left, R: right, Mid: middle, PCC: posterior cingulate cortex, dAIns: dorsal anterior insula, TPJ: temporoparietal junction, dACC: dorsal anterior cingulate cortex.
* $p < 0.05$.

correlated with the general psychopathology subscale score of PANSS ($r = 0.695$, $p = 0.004$) and the PANSS total scores ($r = 0.662$, $p = 0.007$) in the SCH group. Furthermore, the causal connectivity from the right angular to the right DLPFC was negatively correlated with positive subscale scores of PANSS ($r = -0.561$, $p = 0.030$) and the PANSS total scores ($r = -0.539$, $p = 0.038$). In addition, the causal connectivity of the PCC to the right TPJ was positively correlated with disease duration ($r = 0.586$, $p = 0.022$) in the DEP group.

4. Discussion

The triple network model with regard to the DMN, CEN and SN has been considered as a core aspect of psychiatric disorders (Menon 2011). The current study investigated both the functional and effective connectivity across these core networks among patients with SCH and DEP as well as HC during the resting state. The major findings are as follows. (1) Compared with HC, the causal connectivity between the key nodes of the DMN and SN exhibited identical abnormal changes in the two patient groups. The outflow of the PCC to the nodes in the SN was increased in both patients groups compared with HC. (2) Patients with SCH and those with DEP showed completely opposing altered FC patterns of the DMN-CEN and SN-CEN. Compared with HC, the FC between the CEN and DMN was enhanced in patients with SCH but decreased in those with DEP. Conversely, patients with DEP showed increased FC between the CEN and SN whereas those with SCH showed decreased FC. These findings suggest both common and distinct aberrant connectivity patterns across the three networks within the two patient groups (Fig. 3).

4.1. Identical abnormal causal connectivity

Using the PCC as a key node of the DMN, the differences of causal influence with the dAIns and TPJ were observed in the SCH, DEP and HC groups. Interestingly, both patients with SCH and those with DEP showed significantly consistent abnormal changes in the connectivity of the PCC from/to dAIns and TPJ. No significant difference was found between the two patient groups. This identical aberrant causal influence between the PCC and dAIns/TPJ may reflect the parallel deficits of the dynamic interaction between the DMN and SN in the two disorders.

In clinical practice, impairments of the DMN and SN are associated with performance deficits on cognitive and affective tasks among patients with SCH or DEP (Whitfield-Gabrieli et al. 2009). For example, some studies have reported that DMN nodes are typically associated with autobiographical memory (Dastjerdi et al. 2011), episodic memory retrieval (Sestieri et al. 2011) and semantic memory (Binder et al. 2009). Abundant evidences emphasize that the insula, a key node of SN, plays an important role in affective learning and decision making (Singer et al. 2009). In addition, Moran et al. (2013) have implicated that the disrupted AIns modulation of the DMN contributes to deficits in sustained attention, a consistently observable cognitive deficit in both patients with SCH and those with DEP (Park et al. 2012). In particular, the directed path coefficient from the dAIns to nodes in DMN is significantly correlated with rapid visual information processing performance, a task linked to working memory (Wesnes and Warburton 1983). Therefore, the observed parallel aberrant dynamic interaction of the DMN and SN may contribute to the psychopathology of the common cognitive and affective impairments associated with SCH and DEP.

In addition, our results demonstrate that the causal connectivity from the PCC to the TPJ was positively correlated with disease duration among patients with DEP, which provides additional evidence regarding the progressive abnormalities of the dynamic interaction of the brain networks in patients with DEP. However, we did not find an association between this alteration of effective connectivity from PCC to TPJ and the clinical information in patients with SCH. The effect of disease duration should be considered further because previous studies have reported that the structure and FC of the PCC-TPJ are associated with disease duration during the early phase of SCH (Zhang et al. 2014).

4.2. Opposing abnormal functional connectivity

The FC analysis revealed significant group differences among the nodes of the DMN, SN and CEN. Opposite abnormal changes of the FC

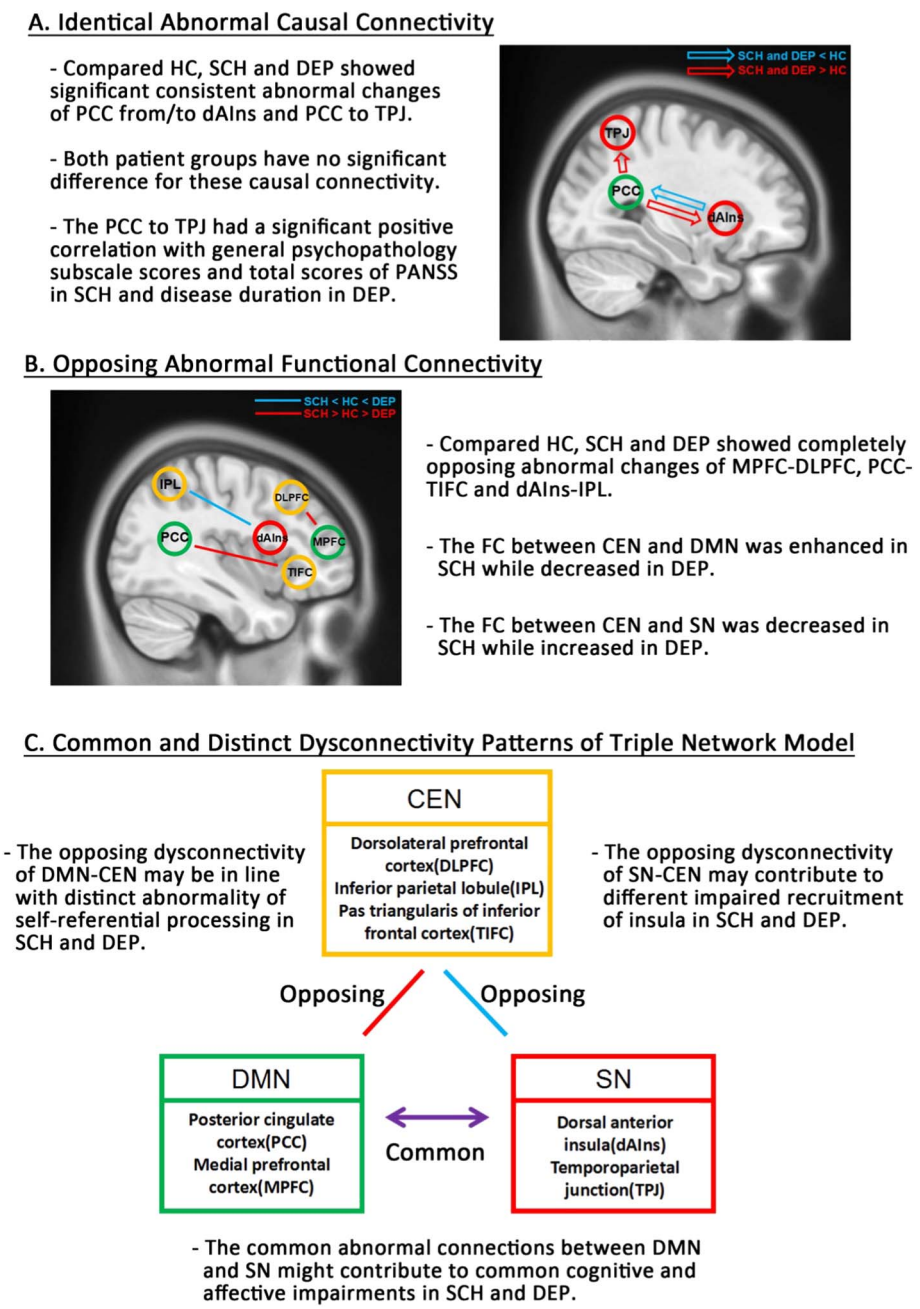

Fig. 3. A model of the common and distinct dysconnectivity patterns of the triple network model with regard to patients with SCH and those with DEP.

between the DMN and CEN (MPFC-DLPFC and PCC-TIFC) were observed in both the SCH and DEP groups. Specifically, compared with HC, SCH patients had a significantly increased positive correlation whereas patients with DEP showed a significantly decreased negative correlation. This result indicates an opposite dysfunctional connectivity pattern for the two psychiatric disorders. Consistent with the opposing alteration between SCH and DEP, a recent meta-analysis on hypoactivation and hyperactivation at rest in patients with SCH and DEP patients found opposing resting-state activity in the ventral MPFC for the both disorders (Kuhn and Gallinat 2013). These opposing dysfunctional connectivity patterns between the DMN and CEN may be in accordance with the distinct process of abnormal self-referential, a core characteristic of SCH and DEP. The key nodes of the DMN, particularly the MPFC and PCC, play crucial roles in different aspects of self-referential processing. The MPFC is typically relative to self-evaluations, social cognitive processes and the self-reference effect of memory (Macrae et al. 2004). Furthermore, the PCC is differentially associated with the autobiographical memory related to internal thought (Dastjerdi et al. 2011). Moreover, the increased FC of DMN-CEN in patients with SCH may be related to reductions in self-referential mental activity. One meta-analysis emphasized the importance of the MPFC in tagging information and decision-making processes relevant for the self (van der Meer et al. 2010). Patients with SCH have shown less self-referential source memory but intact external source memory relative to controls (Fisher et al. 2008). The decreased FC of the DMN-CEN in DEP patients may be related to excessive rumination and increased self-focus. Increased activity in the medial frontal cortex and altered FC between the DMN and CEN were found in DEP patients during self-referential processing (Lemogne et al. 2009). Additionally, the self-focus associated with DEP may be associated with the lack of inhibition between the DMN and the cognitive control network (Lemogne et al. 2012).

Apart from the opposing dysfunctional connectivity between the DMN and CEN, we found another opposite connection pattern with regard to the SN-CEN: decreased FC of the dAIns-IPL in patients with

SCH and increased FC of the dAIns-IPL in those with DEP. The observed opposing dysfunctional connectivity between the SN and CEN may contribute to the different impaired "switching" function of the SN in integrating external and internal stimuli. As a core part of salience network, the anterior insula plays a crucial role in switching between the DMN and CEN, which involved in externally oriented attention and internally oriented self-related mental processes. Deficits of anterior insula in patients with SCH have been linked to the impaired detection and mapping of salient external and internal stimuli, which contribute to abnormal self-monitoring. Consistent with a prior study (Moran et al. 2013), the current study observed decreased FC between the right anterior insula and CEN in patients with SCH. The decreased dAIns modulation to the CEN may be partly derived from a deficient dAIns control mechanism, which implies an inefficient recruitment between the SN and CEN. Different from patients with SCH, those with DEP showed increased FC, which was consistent with Yuen et al. (2014) that increased FC between the right anterior insula and posterior parietal cortex. Recent study suggested that increased insular connectivity may signify increased sensitivity to salient signals in patients with DEP (Kaiser et al. 2016). Therefore, the increased FC between the SN and CEN in patients with DEP may reflect the excessive recruitment of the SN and CEN when processing the external stimuli.

4.3. Limitations

Although a sample size of twenty participants have been reported to prove sufficient statistical power for fMRI studies (Thirion et al. 2007), a larger sample is needed to the increase the reliability and sensitivity to differences with smaller effect size in the future. In addition, all of the patients with SCH or DEP were taking psychotropic medications. Medication use almost perfectly aligned with their diagnostic categories; therefore, it is impossible to disentangle diagnosis from medication effects in the findings. Interpretations of the group differences should be made with caution. The medicated patients were in stable condition, this may have an impact on the functional connectivity of networks. Another limitation is that the psychometric assessments differed between the three groups (none for healthy controls, PANSS for SCH and HAMD for DEP), which precludes any dimensional analysis of the findings across the diagnostic groups. Furthermore, the neuropsychological assessment was not evaluated in the present study. Thus, we can only infer that the altered connectivity is related to patients' general pathophysiologies. The Granger analysis of fMRI data remains controversial because the lagged effects of the BOLD signal are too slow for realistic neural model. Therefore, the results from Granger analysis should be cautiously interpreted. In addition, the "common dysfunction" (when the two patients group differ from the healthy controls, but not from each other) is limited to small sample sizes. Finally, a limitation of all resting-state studies is that patients and healthy participants may not be entirely at rest, although they were instructed to keep their minds wander.

5. Conclusion

Using both FC and Granger causal analysis, the current study observed identical and opposite aberrant connectivity patterns across three core networks (DMN, SN and CEN) between patients with SCH and those with DEP. Intriguingly, the causal connectivity between the key nodes of the DMN and SN showed identical abnormal changes in the two patient groups, which may contribute to the psychopathologies of the common cognitive and affective impairments associated with SCH and DEP. Interestingly, both SCH and DEP patient groups showed opposing changes of dysfunctional connectivity of the DMN-CEN and SN-CEN. The opposing dysfunctional connectivity patterns of the DMN-CEN may be in line with different abnormalities of self-referential processing, a prototypical but distinct manifestation of SCH and DEP. Finally, the observed opposing dysfunctional connectivity between the SN and CEN may contribute to the different impaired recruitment between the SN and CEN.

Ethical statement

The study was approved by the Ethics Committee of Chengdu Mental Health Center, Chengdu, China. Written informed consent was obtained after a complete description of the study for each participant.

Conflict of interest

There is no conflict of interest.

Contributors

Y. Jiang, M. Duan, C. Luo and D. Yao designed the study and wrote the protocol. X. Chang, X. Chen and Y. Li managed the literature searches and analyses. Y. Jiang and H. He undertook the statistical analysis. Y. Jiang and M. Duan wrote the first draft of the manuscript. All authors contributed to and have approved the final manuscript.

Acknowledgments

This study was supported by the National Nature Science Foundation of China (No. 81330032, 81471638, 81571759), Special-Funded Program on National Key Scientific Instruments and Equipment Development of China (No. 2013YQ490859), The Chinese Fundamental Research Funding for Central Universities in UESTC (ZYGX2015J091, ZYGX2016J124), and the Sixth Science and Technology Project (2013) from the Chengdu Science and Technology Bureau (No. 2013-11).

Appendix A. Supplementary data

Supplementary data to this article can be found online at http://dx.doi.org/10.1016/j.pnpbp.2017.07.007.

References

Binder, J.R., Desai, R.H., Graves, W.W., Conant, L.L., 2009. Where is the semantic system? A critical review and meta-analysis of 120 functional neuroimaging studies. Cerebral cortex 19 (12), 2767–2796.

Cao, W., Cao, X., Hou, C., Li, T., Cheng, Y., Jiang, L., Luo, C., Li, C., Yao, D., 2016. Effects of cognitive training on resting-state functional connectivity of default mode, salience, and central executive networks. Front Aging Neurosci 8, 70.

Chai, X.J., Castanon, A.N., Ongur, D., Whitfield-Gabrieli, S., 2012. Anticorrelations in resting state networks without global signal regression. NeuroImage 59 (2), 1420–1428.

Chen, G., Glen, D.R., Saad, Z.S., Paul Hamilton, J., Thomason, M.E., Gotlib, I.H., Cox, R.W., 2011. Vector autoregression, structural equation modeling, and their synthesis in neuroimaging data analysis. Computers in biology and medicine 41 (12), 1142–1155.

Chen, X., Duan, M., He, H., Yang, M., Klugah-Brown, B., Xu, H., Lai, Y., Luo, C., Yao, D., 2016. Functional abnormalities of the right posterior insula are related to the altered self-experience in schizophrenia. Psychiatry Res. 256, 26–32.

Chen, X., Liu, C., He, H., Chang, X., Jiang, Y., Li, Y., Duan, M., Li, J., Luo, C., Yao, D., 2017. Transdiagnostic differences in the resting-state functional connectivity of the prefrontal cortex in depression and schizophrenia. J. Affect Disord. 217, 118–124.

Dastjerdi, M., Foster, B.L., Nasrullah, S., Rauschecker, A.M., Dougherty, R.F., Townsend, J.D., Chang, C., Greicius, M.D., Menon, V., Kennedy, D.P., Parvizi, J., 2011. Differential electrophysiological response during rest, self-referential, and non-self-referential tasks in human posteromedial cortex. Proceedings of the National Academy of Sciences of the United States of America 108 (7), 3023–3028.

Dong, D., Wang, Y., Chang, X., Luo, C., Yao, D., 2017. Dysfunction of large-scale brain networks in schizophrenia: a meta-analysis of resting-state functional connectivity. Schizophr Bull (sbx034).

Duan, M., Chen, X., He, H., Jiang, Y., Jiang, S., Xie, Q., Lai, Y., Luo, C., Yao, D., 2015. Altered basal ganglia network integration in schizophrenia. Front Hum. Neurosci. 9, 561.

Fisher, M., McCoy, K., Poole, J.H., Vinogradov, S., 2008. Self and other in schizophrenia: a cognitive neuroscience perspective. The American journal of psychiatry 165 (11), 1465–1472.

Fox, M.D., Snyder, A.Z., Vincent, J.L., Corbetta, M., Van Essen, D.C., Raichle, M.E., 2005. The human brain is intrinsically organized into dynamic, anticorrelated functional networks. Proceedings of the National Academy of Sciences of the United States of

America 102 (27), 9673–9678.
Hamilton, J.P., Chen, G., Thomason, M.E., Schwartz, M.E., Gotlib, I.H., 2011. Investigating neural primacy in major depressive disorder: multivariate Granger causality analysis of resting-state fMRI time-series data. Molecular Psychiatry 16 (7), 763–772.
Kaiser, R.H., Whitfield-Gabrieli, S., Dillon, D.G., Goer, F., Beltzer, M., Minkel, J., Smoski, M., Dichter, G., Pizzagalli, D.A., 2016. Dynamic resting-state functional connectivity in major depression. Neuropsychopharmacology 41 (7), 1822–1830.
Kuhn, S., Gallinat, J., 2013. Resting-state brain activity in schizophrenia and major depression: a quantitative meta-analysis. Schizophrenia Bull. 39 (2), 358–365.
Lemogne, C., le Bastard, G., Mayberg, H., Volle, E., Bergouignan, L., Lehericy, S., Allilaire, J.F., Fossati, P., 2009. In search of the depressive self: extended medial prefrontal network during self-referential processing in major depression. Social Cognitive and Affective Neuroscience 4 (3), 305–312.
Lemogne, C., Delaveau, P., Freton, M., Guionnet, S., Fossati, P., 2012. Medial prefrontal cortex and the self in major depression. Journal of Affective Disorders 136 (1-2), e1–e11.
Luo, C., Li, Q., Lai, Y., Xia, Y., Qin, Y., Liao, W., Li, S., Zhou, D., Yao, D., Gong, Q., 2011. Altered functional connectivity in default mode network in absence epilepsy: a resting-state fMRI study. Hum. Brain Mapp. 32 (3), 438–449.
Macrae, C.N., Moran, J.M., Heatherton, T.F., Banfield, J.F., Kelley, W.M., 2004. Medial prefrontal activity predicts memory for self. Cerebral Cortex 14 (6), 647–654.
van der Meer, L., Costafreda, S., Aleman, A., David, A.S., 2010. Self-reflection and the brain: a theoretical review and meta-analysis of neuroimaging studies with implications for schizophrenia. Neuroscience and Biobehavioral Reviews 34 (6), 935–946.
Menon, V., 2011. Large-scale brain networks and psychopathology: a unifying triple network model. Trends in Cognitive Sciences 15 (10), 483–506.
Menon, V., Uddin, L.Q., 2010. Saliency, switching, attention and control: a network model of insula function. Brain Structure & Function 214 (5-6), 655–667.
Moran, L.V., Tagamets, M.A., Sampath, H., O'Donnell, A., Stein, E.A., Kochunov, P., Hong, L.E., 2013. Disruption of anterior insula modulation of large-scale brain networks in schizophrenia. Biological Psychiatry 74 (6), 467–474.
Nekovarova, T., Fajnerova, I., Horacek, J., Spaniel, F., 2014. Bridging disparate symptoms of schizophrenia: a triple network dysfunction theory. Frontiers in Behavioral Neuroscience 8, 171.
Palaniyappan, L., Simmonite, M., White, T.P., Liddle, E.B., Liddle, P.F., 2013. Neural primacy of the salience processing system in schizophrenia. Neuron 79 (4), 814–828.
Park, S.H., Noh, J.C., Kim, J.H., Lee, J., Park, J.Y., Lee, Y.R., Kim, C.H., Lee, K.H., 2012. Interactive effects of background facial emotion stimulus and target salience on sustained attention performance in schizophrenia. Schizophrenia Research 135 (1-3), 90–94.
Pessoa, L., 2008. On the relationship between emotion and cognition. Nature Reviews. Neuroscience 9 (2), 148–158.
Power, J.D., Barnes, K.A., Snyder, A.Z., Schlaggar, B.L., Petersen, S.E., 2012. Spurious but systematic correlations in functional connectivity MRI networks arise from subject motion. NeuroImage 59 (3), 2142–2154.
Saad, Z.S., Gotts, S.J., Murphy, K., Chen, G., Jo, H.J., Martin, A., Cox, R.W., 2012. Trouble at rest: how correlation patterns and group differences become distorted after global signal regression. Brain Connectivity 2 (1), 25–32.
Satterthwaite, T.D., Elliott, M.A., Gerraty, R.T., Ruparel, K., Loughead, J., Calkins, M.E., Eickhoff, S.B., Hakonarson, H., Gur, R.C., Gur, R.E., Wolf, D.H., 2013. An improved framework for confound regression and filtering for control of motion artifact in the preprocessing of resting-state functional connectivity data. NeuroImage 64, 240–256.
Seeley, W.W., Menon, V., Schatzberg, A.F., Keller, J., Glover, G.H., Kenna, H., Reiss, A.L., Greicius, M.D., 2007. Dissociable intrinsic connectivity networks for salience processing and executive control. The Journal of Neuroscience 27 (9), 2349–2356.
Sestieri, C., Corbetta, M., Romani, G.L., Shulman, G.L., 2011. Episodic memory retrieval, parietal cortex, and the default mode network: functional and topographic analyses. The Journal of Neuroscience 31 (12), 4407–4420.
Sheline, Y.I., Barch, D.M., Price, J.L., Rundle, M.M., Vaishnavi, S.N., Snyder, A.Z., Mintun, M.A., Wang, S., Coalson, R.S., Raichle, M.E., 2009. The default mode network and self-referential processes in depression. Proc Natl Acad Sci U S A 106 (6), 1942–1947.
Singer, T., Critchley, H.D., Preuschoff, K., 2009. A common role of insula in feelings, empathy and uncertainty. Trends in cognitive sciences 13 (8), 334–340.
Thirion, B., Pinel, P., Tucholka, A., Roche, A., Ciuciu, P., Mangin, J.F., Poline, J.B., 2007. Structural analysis of fMRI data revisited: improving the sensitivity and reliability of fMRI group studies. IEEE transactions on medical imaging 26 (9), 1256–1269.
Touroutoglou, A., Hollenbeck, M., Dickerson, B.C., Feldman Barrett, L., 2012. Dissociable large-scale networks anchored in the right anterior insula subserve affective experience and attention. NeuroImage 60 (4), 1947–1958.
Wesnes, K., Warburton, D.M., 1983. Effects of smoking on rapid information processing performance. Neuropsychobiology 9 (4), 223–229.
Whitfield-Gabrieli, S., Ford, J.M., 2012. Default mode network activity and connectivity in psychopathology. Annual Review of Clinical Psychology 8, 49–76.
Whitfield-Gabrieli, S., Thermenos, H.W., Milanovic, S., Tsuang, M.T., Faraone, S.V., McCarley, R.W., Shenton, M.E., Green, A.I., Nieto-Castanon, A., LaViolette, P., Wojcik, J., Gabrieli, J.D., Seidman, L.J., 2009. Hyperactivity and hyperconnectivity of the default network in schizophrenia and in first-degree relatives of persons with schizophrenia. Proceedings of the National Academy of Sciences of the United States of America 106 (4), 1279–1284.
Yuen, G.S., Gunning-Dixon, F.M., Hoptman, M.J., AbdelMalak, B., McGovern, A.R., Seirup, J.K., Alexopoulos, G.S., 2014. The salience network in the apathy of late-life depression. International Journal of Geriatric Psychiatry 29 (11), 1116–1124.
Zang, Z.X., Yan, C.G., Dong, Z.Y., Huang, J., Zang, Y.F., 2012. Granger causality analysis implementation on MATLAB: a graphic user interface toolkit for fMRI data processing. Journal of Neuroscience Methods 203 (2), 418–426.
Zhang, F., Qiu, L., Yuan, L., Ma, H., Ye, R., Yu, F., Hu, P., Dong, Y., Wang, K., 2014. Evidence for progressive brain abnormalities in early schizophrenia: a cross-sectional structural and functional connectivity study. Schizophrenia Research 159 (1), 31–35.